

# Patterns of Transformations in the Compositions and Properties of Icelandic Hyaloclastites during Lithogenesis

Yu. V. Frolova

Faculty of Geology, Department of Engineering and Ecological Geology, Moscow State University

e-mail: skalka@geol.msu.ru

Received June 18, 2009

**Abstract**—In Iceland, hyaloclastites form thick masses generated as a result of subglacial eruptions during Pliocene–Pleistocene surface glaciations. The formation of hyaloclastites and features of their alterations during lithogenesis were investigated. Hyaloclastites are extremely heterogeneous in their physical and physical–mechanical properties. A sequence of hyaloclastites secondary transformations was established from virgin, only slightly palagonitized hyaloclastites with contact-type cement to thoroughly transformed rocks with secondary minerals forming porous cement and partially substituting volcanic glass. A general tendency towards an increase in elasticity, density, strength, and thermal characteristics and towards a decrease in porosity and permeability has been observed with progression of secondary alterations, with the growth of age, from newer to more ancient deposits, and the depth of hyaloclastite burial.

*Key words:* hyaloclastites, secondary alteration, palagonite, Iceland, physical–mechanical properties.

**DOI:** 10.3103/S0145875210020067

## INTRODUCTION

The patterns of generation and properties of various types of grounds are currently in the focus of modern soil science. Until recently in the general classification three subgroups have been identified, namely magmatic, metamorphic and sedimentary. In the most recent classification a new subgroup of volcanogenic–sedimentary grounds has been introduced [*Gruntovedenie...*, 2005], which, however have stayed mostly out of focus of engineering geology, as previously. Tuffs and tuffites are the most abundant volcanogenic–sedimentary rocks. Clastolavas, lavoclastites, agglutinates, ignimbrites, and hyaloclastites are less abundant formations and therefore very poorly studied. Still, in areas of modern or ancient volcanism such rocks are common and serve as a basement or enclosing medium for various engineering structures.

The results of investigation of hyaloclastites, volcanogenic–sedimentary rocks with highly specific features, are under consideration in this paper. Such rocks are generated beneath the water or ice surface during phreatic eruptions. Upon contact with water lava cools rapidly, turning into small fragments of volcanic glass, which get cemented later under the influence of various postgenetic processes. The resulting deposits are usually thick and generally look like tuffs forming on the ground. However, unlike tuffs, hyaloclastite fragments are mainly volcanic glass. Hyaloclastites are abundant on the ocean floor and on the continents in mountain systems in places where basaltic volcanism once occurred concurrently with glaciation.

In particular, thick masses of hyaloclastite can be observed on vast territories in Iceland. These were formed during the Pliocene–Pleistocene glaciations. Interest in hyaloclastites was increased by the development of geothermal power engineering. As highly porous and permeable materials, hyaloclastites are widely used as collectors of thermal water in Iceland in heating and electric power supply systems. Knowledge of the physical and physical–mechanical properties of hyaloclastites is of significance in tackling a variety of practical problems, e.g., in assessing geothermal tank efficiency and durability, drilling exploratory and production wells, and building geothermal power stations. Hyaloclastites are of much interest for scientists as an object generated in specific conditions, viz., phreatic eruptions beneath the sea surface or, as in Iceland, under the ice.

The process of hyaloclastite generation and lithification is widely covered in scientific literature, predominantly foreign; however, scientists have not arrived at a consensus so far as regards the mechanisms of their formation and alteration [Hay, Iijima, 1968; Jakobsson, Moore, 1986; Zhou, Fyfe, 1989; Jercinovic et al., 1990; Crovisier et al., 1992; Thorseth et al., 1998; Schiffman et al., 2000]. Research focuses more on geochemical and mineralogical aspects rather than changes in hyaloclastite structure and properties during postgenetic processes. The papers by Russian scientists containing the most comprehensive data on the chemical and mineral composition of Icelandic hyaloclastites and their lithogenic transformations are

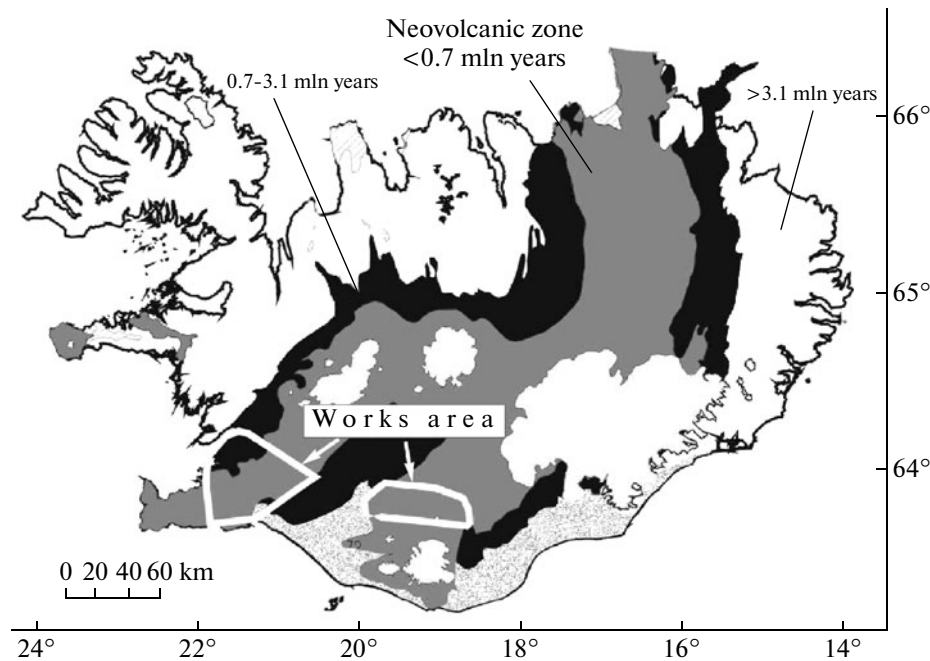


Fig. 1. Geological map of Iceland with indication of works area.

Geptner [1977] and Geptner et al. [1984]. In these papers the authors demonstrate that hyaloclastite cementation and transformation occur in a wide range of conditions. On the land they can appear in a zone of weathering and transformation of material in ice conditions, on the bottom of fresh and salt water reservoirs. Buried masses of hyaloclastites undergo changes under the action of cold or thermal groundwater.

### GEOLOGICAL CONDITIONS

As a region with one of the highest eruptive activities, Iceland is an adequate place to study volcanogenic and volcanogenic–sedimentary rocks and their properties. The island is situated at the intersection of the Mid-Atlantic Ridge and sublatitudinal North Ridge (the Greenland–Iceland and Faroe–Iceland Ridges) and has been a zone of active volcanism since the Miocene [Ghenshaft, Saltykovskii, 1999].

In all, four complexes of volcanites have been identified (Fig. 1): Miocene (16–3.1 Ma ago), Pliocene–Eopleistocene (0.7–3.1 Ma ago), Upper Pleistocene (from 0.7 Ma to 9–13 Ma years ago) and Holocene (younger than 9000–13000 years ago) [Saemundsson, 1979]. In the Miocene stage of volcanism a massive plateau basalt thickness was formed covering over half of Iceland's territory. Fissure eruptions were accompanied by the formation of complex central-type volcanoes. In two later stages, subaerial and subglacial eruptions alternated, giving rise to so-called hyaloclastite formation, which includes hyaloclastite tuffs, breccias, and pillow-lavas. Since the Upper Pleistocene, volcanic activity has been localized in the neovolcanic zone.

Pliocene–Pleistocene hyaloclastites are the focus of the present study. The hyaloclastite formation developed as a result of subglacial phreatic eruptions, a common Pliocene–Pleistocene phenomena, during cover glaciations. As a rule, hyaloclastites form extended ridges and distinctive forms of relief called mesas or tuyas composed of underlying pillow lavas rimmed with breccias and hyaloclastite tuffs. In some cases, the lava that erupted under the ice melted a glacier and burst through it onto the surface with the formation of lava covers overlaying breccias and tuffs and armoring the mesas. The conditions and mechanism of generation of hyaloclastite formations are described in detail in Jones [1970].

### METHODS OF RESEARCH

Samples for the study (75 samples) were taken in the south and southwest of Iceland. The collection includes hyaloclastites dated to different times (the latest glaciation  $Q_3$ , 0.7–1, 1.7–2, and 2.5 Ma ago) and buried at different depths (not buried, 500, 700, and 1000 m) [Frolova et al., 2005]. The core samples were taken with the use of a portable drilling unit. In each sampling site, several samples were taken. In the laboratory the properties of such samples were measured concurrently, followed by calculation of averages.

Measurements were made to determine the physical and physical-mechanical parameters as follows: density ( $\rho$ ); solid phase density (mineral density, specific weight) ( $\rho_s$ ); porosity, general ( $n$ ), water-filled porosity ( $n_{\text{wat}}$ ), air-filled porosity ( $n_{\text{air}}$ ); gas permeabil-

ity ( $K$ ); hygroscopic moisture ( $W_r$ ); velocity of longitudinal wave propagation ( $V_p$ ); uniaxial compression resistance ( $R_c$ ); and magnetic susceptibility ( $\chi$ ). The measurements were performed by standard techniques on cylindrical samples ( $H \geq D = 2.5$  cm) [Trofimov, Korolev, 1993]. Thermal characteristics, such as the coefficients of thermal conductivity ( $\gamma$ ) and diffusivity ( $\alpha$ ) were determined by V.G. Popov (13 measurements) at the Faculty of Physics of Moscow State University; gas permeability (24 measurements) was determined by V. P. Shustrov of Podzemgasprom Ltd. [GOST..., 1985].

Cluster analysis was performed to clarify the petro-physical heterogeneity of hyaloclastites and to identify homogeneous groups. The  $K$ -mean-value method was applied as follows:  $k$  clusters (groups) were taken at random, allocation of samples to clusters was changed so that the variance within the clusters was minimal and the variance between the clusters was maximal. A description was made and average values of the properties were calculated for each cluster. At total of eight parameters, such as density, solid-phase density, porosity (general, water- and air-filled), hygroscopic moisture, velocity of longitudinal wave propagation, and resistance were used as a base for the cluster analysis. Prior to clusterization all the quantities were standardized:

$$Z_i = (X_i - X_{iav})/S_i,$$

where  $Z_i$  is a standardized quantity and  $S_i$ ,  $X_{iav}$  are the standard deviation and mean value of  $X_i$ , respectively.

The cluster analysis revealed five groups (clusters), which were homogeneous by properties. The groups were juxtaposed with geological and petrographic factors.

Concurrently with the definition of properties, the composition and structure of the rocks were investigated. Description of all the samples was made on the basis of macroscopic thin and polished section examination. Mineral composition was determined for 11 samples using a DRON-6 X-ray diffractometer (analyst V.G. Shlykov<sup>†</sup>). The composition of clayey minerals was studied in more detail under heating of the samples to 500°C and glycerin saturation. Some of the samples were investigated by electron microscopy to determine their chemical composition on a Camebax SX-50 microanalyzer (six samples, 42 tests).

## RESULTS AND DISCUSSION

### *General Characteristics of Hyaloclastites*

**Mineral composition and structure.** The hyaloclastites under investigation are detrital vitreous rocks composed of angular, sharp (less frequently, rounded), porous, and optically isotropic volcanic glass fragments cemented with secondary minerals. Crystallite of olivine, pyroxene and plagioclase are present

in insignificant quantities. Only hyaloclastites of psammitic and fine psephitic structure were selected for measurements of the properties; therefore, the sizes of the fragments of the examined samples range from 0.01 to 1 cm.

Volcanic glass of basalt (tholeit) composition is a major constituent of hyaloclastites. It is a thermodynamically unstable and readily transformable material. Basalt glass reacts rapidly with cold and thermal fluids, thereby undergoing chemical and mineral transformations accompanied by changes in pore space structure and permeability and of all properties. All hyaloclastite samples were altered, albeit to a varying degree. Palagonite is a product that is generated first during volcanic glass transformation. The term "palagonite" was first used by Walterhausen in 1845 in his description of hyaloclastites of Palagonia in Sicily island [Stroncik, Shmincke, 2001]. In scientific literature the term "palagonite" is commonly used for any hydrated product substituting mafic volcanic glass as well as for any crystalline material in a palagonite matrix. Usually two types of palagonites are distinguished: (1) yellow, optically isotropic pure "gel-palagonite" and (2) yellowish-brown, slightly optically anisotropic, double-refracting fibrous or stratified palagonite (fibropalagonite), which is generated on the outer surface of gel-palagonite in later stages of palagonitization. The second type of palagonite has been shown to be simply an incipient clayey mineral, smectite, whereas palagonite proper is an x-ray amorphous substance. Palagonitization is described in many scientific articles. Various palagonitization mechanisms have been suggested, mainly metasomatism, dissolution of volcanic glass with further deposition within the same boundaries (without volume change), and deposition on the surface of glass fragment (with volume change).

All the samples tested were shown to be palagonitized, albeit to a considerably varying degree. Palagonite usually forms "skirts" on the surface of volcanic glass fragments. It also forms on the inner surfaces of some gas pores in volcanic glass and in feeder micro cracks. Closed gas cavities not communicating with interclastic space by micro cracks remain empty (Fig. 2a). The microscopic structure of various palagonite generations and the "skirts" differs.

The boundary (interface) between the volcanic glass and palagonite can be of different types (Fig. 2). A sharp boundary is typical for most samples (Fig. 2b). The chemical composition of the glass fragments is identical for the fragment's central part and rims and changes abruptly in the zone of transition to palagonite (Fig. 3a, Table 1). In some cases traces of leaching several microns thick can be observed (Fig. 3b). Boundaries of the dendritic type are occasionally observed (Fig. 2c). Dark dendritic "branches" penetrate into the virgin volcanic glass. According to Crovisier et al., [1992], the type of boundary depends on conditions and the speed of transformation. Micro

<sup>†</sup>Deceased.

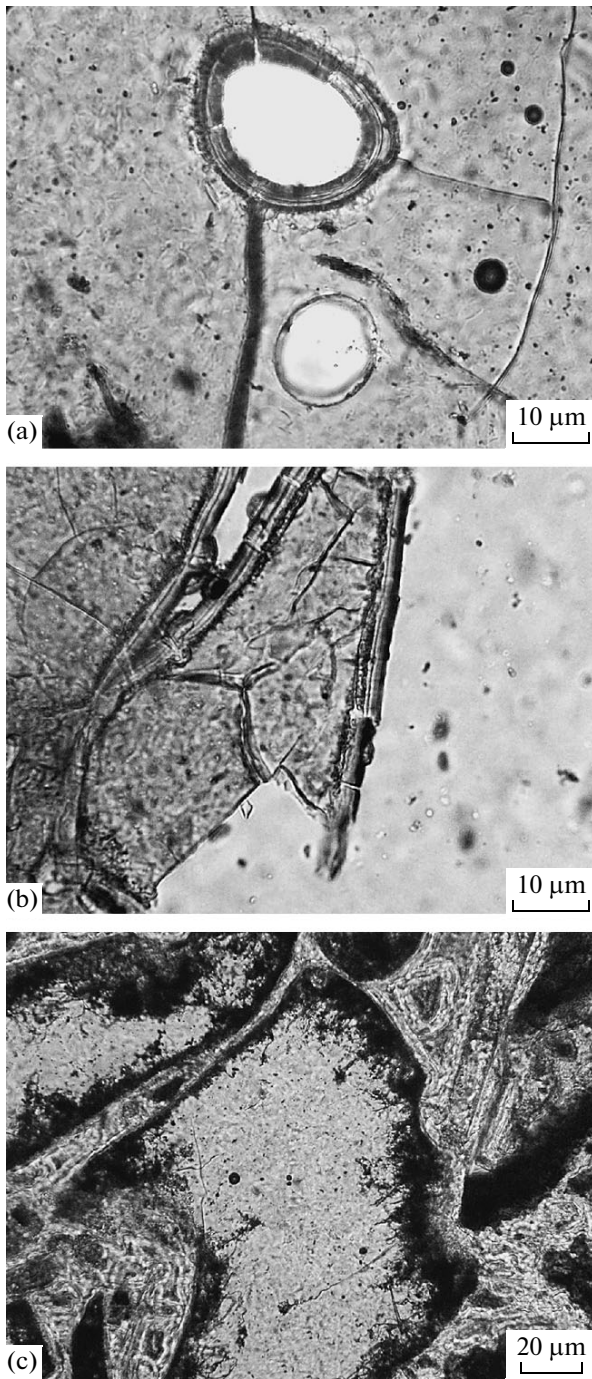


**Fig. 2.** Mechanism of palagonite development: (a) formation of palagonite on pore surface on a glass matrix with a feeder micro crack; (b, c) glass-palagonite boundary ((b) sharp boundary, (c) “dendriticundary”).

cracks on the glass-palagonite interface enhance permeability and, consequently, further alterations.

The chemical composition of volcanic glass and palagonite differs significantly (Table 1). According to microprobe analysis data, palagonitization is accompanied by the carryover of most petrogenic elements as manifested by a notable reduction of Si, Mg, Ca, and

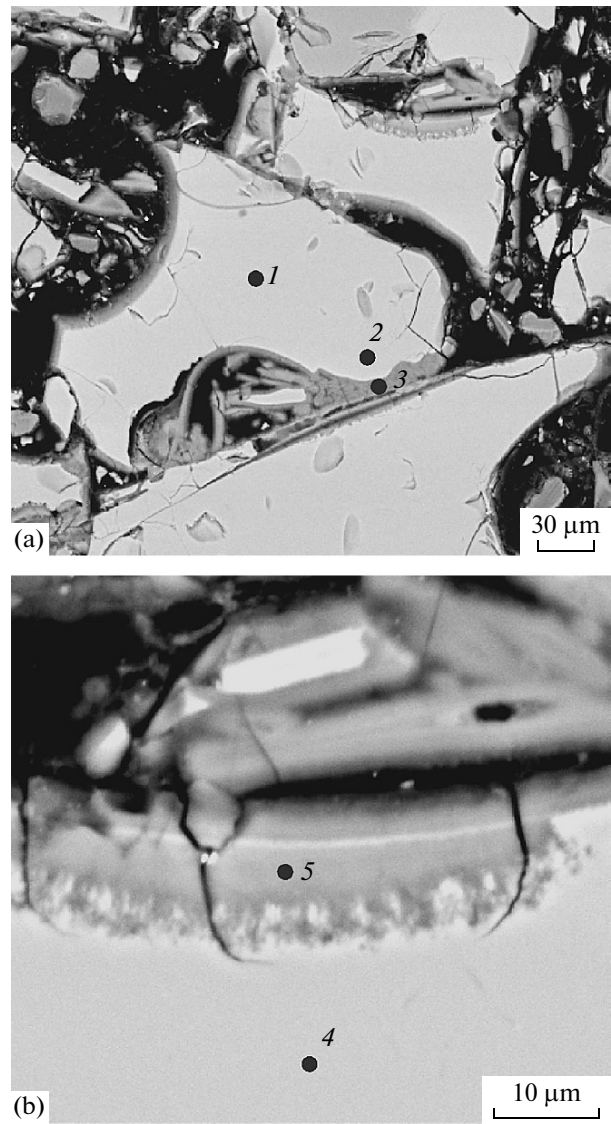


**Fig. 3.** Initial stage of palagonitization: (a) palagonite at contact with glass fragment; (b) leaching zone and palagonitization on the rim of the glass fragment (electron microscopy). Chemical composition for points 1–5 is given in Table 1.

Na, as well as insignificant reductions of Al, Fe, and K, while Ti is not removed. All elements in palagonite total 82–85 wt %. Water accounts for the difference from 100 wt %, as first shown in Stroncik, Schmincke [2001] based on infrared colorimetry results.

From the viewpoint of engineering geology, palagonitization is of interest because the process leads to cementation of loose volcanogenic and sedimentary deposits with the formation of consolidated rocks or, in other words, rock grounds. Rapid palagonitization is, as a rule, accompanied by the deposition of authigenic minerals, such as zeolites, clays, and calcite in the pores and interclastic space. Petrographical and geochemical studies (in thin sections, X-ray structure

**Table 1.** Chemical composition of volcanic glass and palagonite (microanalysis data), wt %

Point number	SiO <sub>2</sub>	TiO <sub>2</sub>	Al <sub>2</sub> O <sub>3</sub>	FeO	MnO	MgO	CaO	Na <sub>2</sub> O	K <sub>2</sub> O	SO	ClO	Σ
Glass, fragment center	48.521	1.398	15.922	10.837	0.119	8.370	13.084	2.154	0.145	0.079	0.022	100.651
Glass, fragment rim	48.159	1.304	15.529	10.964	0.128	8.726	12.46	2.202	0.208	0.0183	0.24	100
Palagonite at fragment contact	44.097	1.613	13.789	9.772	0.221	5.316	7.277	0.055	0.065	0.019	0.038	82.262
Glass, fragment center	49.405	1.338	15.777	10.581	0.142	8.362	12.832	2.099	0.124	0.049	0.017	100.726
Rim of palagonite	45.832	1.68	14.016	9.578	0.134	5.08	8.729	0.262	0.123	0.042	0	85.476

\* See Fig. 3.

analysis, and SEM) made it possible to identify the fundamental stages of transformation from unaltered or slightly palagonitized hyaloclastites to drastically altered hyaloclastites with secondary minerals generated in interclastic space and on the glass matrix. The description and comparison of properties for such stages are given below.

**Properties of hyaloclastites.** Hyaloclastites are characterized by extremely varied properties. There are both weakly cemented varieties, which are highly porous and permeable ( $\rho = 1.2\text{--}1.3\text{ g/cm}^3$ ,  $n = 50\text{--}55\%$ ,  $K = 6.4 \times 10^3\text{ mD}$ ), and dense varieties with low porosity and permeability ( $\rho = 2.1\text{--}2.3\text{ g/cm}^3$ ,  $n = 14\%$ ,  $K = 0.001\text{ mD}$ ). For most samples the solid phase density is  $2.7\text{--}2.9\text{ g/cm}^3$ , (up to  $3.07\text{ g/cm}^3$ ), corresponding to rocks of a basalt composition. The hygroscopic moisture, which reflects the contents of the clayey minerals and palagonite ranges from 0.4 to 13%. The velocity of longitudinal wave propagation varies within 0.9–4.05 km/s, in water saturated samples it is slightly elevated to 1.15–4.3 km/s while the uniaxial compressive resistance changes by two orders, from a few MPa to 100 MPa. The magnetic susceptibility of hyaloclastites is predominantly low and ranges from  $(0.4\text{ to }5) \times 10^{-3}$  SI units, but is high (over  $30 \times 10^{-3}$  SI units) in some samples. The coefficient of heat conductivity is abnormally low as compared to other rock grounds and ranges from 0.37 to 1.33 W/(m K) [Popov et al., 2006]. Since heat conductivity of basalt glass is considerably higher on the average  $\lambda$  is 1.5 W/(m K) [Dortman, 1984] low heat conductivity of hyaloclastites is due to their high porosity, clastic structure, and poor fragments cementation.

The large variation of hyaloclastite properties is mainly due to the different extents of secondary alterations in the course of postgenetic processes. Cluster analysis was carried out to elucidate the nature of such variations and to identify groups of rocks homogeneous by their properties. Based on the results of the cluster analysis, five groups that are homogeneous in their properties have been identified. The properties of rocks from each group are shown in Table 2. The

groups identified by cluster analysis were juxtaposed with geological factors, such as the petrography of the rocks, secondary alterations, age, and depth of thickness burial.

Such juxtaposition revealed a good correlation between the groups and stages of postgenetic transformations. Each group turns out to be characterized by its type of cement and a set of secondary minerals and corresponds to a particular stage of conversion. In addition to correlation with the stage of conversion, the separated clusters correspond well with the age and depth of hyaloclastite mass burial. As a result, it was not difficult to sequence and understand the mechanisms of hyaloclastite secondary alterations during lithogenesis and recognize the changes in the composition and structure of porous space and the influence of such changes on the physical properties of the rocks. A detailed description of each group is given below (Table 2, Fig. 3).

#### *Description of the Groups Identified by Cluster Analysis*

**Group I** includes hyaloclastites generated during the most recent glaciation, which were not buried during their postgenetic history and remained on the surface. These are dark-brown or, less frequently, yellowish–brown rocks representing the most recent or slightly altered varieties corresponding to initial stage of palagonitization. Palagonite “welds” glass fragments at contact points, forming a contact-type cement (Fig. 4). Glass fragments remain unchanged or are altered slightly on their rims. In the latter case, thin palagonite rims ( $\sim 5\text{ }\mu\text{m}$  or, less frequently, up to  $10\text{ }\mu\text{m}$  thick) occasionally form on the surface of glass fragments. In thin sections, the glass fragments and palagonite appear to be optically isotropic. No secondary minerals with crystalline structure have been detected by X-ray analysis, but only X-ray amorphous substance. As a rule, the boundary between the glass and palagonite is sharp. The area of transition from the glass to palagonite has a content of most petrogenic

**Table 2.** Physical and Physicochemical Properties of Icelandic hyaloclastites

Parameter	Group I*	Group II	Group III	Group IV	Group V
$\rho$ , g/cm <sup>3</sup>	$\frac{1.3-1.6^{**}}{1.49}$	$\frac{1.2-1.46}{1.35}$	$\frac{1.53-1.85}{1.67}$	$\frac{1.85-2.34}{2.03}$	$\frac{2.06-2.18}{2.13}$
$\rho_s$ , g/cm <sup>3</sup>	$\frac{2.72-3.0}{2.84}$	$\frac{2.67-2.83}{2.76}$	$\frac{2.49-2.8}{2.66}$	$\frac{2.45-2.75}{2.57}$	$\frac{2.91-2.92}{2.92}$
$W_h$ , %	$\frac{0.6-4.9}{2.3}$	$\frac{3.8-10.5}{6.5}$	$\frac{2.2-10.5}{5.6}$	$\frac{3.3-10.4}{5.8}$	$\frac{1.5-3.8}{2.3}$
$n$ , %	$\frac{42-54}{48}$	$\frac{45-57}{51}$	$\frac{31-45}{37}$	$\frac{14-27}{21}$	$\frac{25-43}{33}$
$n_{air}$ , %	$\frac{37-52}{43}$	$\frac{39-55}{46}$	$\frac{16-38}{31}$	$\frac{6.5-25}{13}$	$\frac{15-26}{20}$
$n_{air}/n$	$\frac{0.81-1}{0.91}$	$\frac{0.81-0.96}{0.91}$	$\frac{0.52-0.96}{0.82}$	$\frac{0.33-0.9}{0.61}$	$\frac{0.49-0.87}{0.64}$
$n_{water}$ , %	$\frac{21-36}{30}$	$\frac{25-39}{32}$	$\frac{18-30}{24}$	$\frac{9.9-21}{17}$	$\frac{20-24}{22}$
$K$ , mD	$\frac{(0.21-5.98) \times 10^3}{3.3 \times 10^3}$	$\frac{(1.68-6.35) \times 10^3}{3.9 \times 10^3}$	$\frac{(0.4-9.5) \times 10^2}{6.1 \times 10^2}$	$\frac{0.23-203.8}{55.5}$	$\frac{10^{-3}-6 \times 10^{-2}}{0.03}$
$V_p$ , km/s	$\frac{1.25-2.55}{1.75}$	$\frac{0.9-1.55}{1.15}$	$\frac{1.3-2.7}{1.9}$	$\frac{1.3-2.95}{2.05}$	$\frac{2.95-4.05}{3.4}$
$V_{pb}$ , km/s	$\frac{1.85-2.5}{2.05}$	$\frac{1.15-2.1}{1.65}$	$\frac{2.05-2.9}{2.5}$	$\frac{2.65-4.3}{3.35}$	$\frac{2.9-3.75}{3.3}$
$R_c$ , MPa	$\frac{2-13}{7.2}$	$\frac{2-10}{4.4}$	$\frac{8-37}{19}$	$\frac{40-111}{60}$	$\frac{48-99}{70}$

Notes: \* Groups descriptions are given in the text.

\*\* Above the line—indicator's minimal and maximum values, under the line—average value.

elements that is significantly reduced for Si, Mg, Ca, and Na and is slightly reduced for Al, Fe, and K (Table 1). In some cases, a 2–3  $\mu\text{m}$  zone of leaching can be observed on the glass rims (Fig. 3b).

Hyaloclastites of group I are noted for low density ( $\rho = 1.3-1.6 \text{ g/cm}^3$ ) and high porosity ( $n = 42-54\%$ ) and permeability ( $K = 2 \times 10^2-6 \times 10^3 \text{ mD}$ ) due to their clastic structure and the fact that their interclastic pores are not filled with secondary minerals (Table 2). Effective air-filled porosity is close to general porosity, i.e., practically all pores are interconnected ( $n_{air}/n = 0.8-1$ ). On the average, the effective water-filled porosity is 30% lower than the effective air-filled porosity. Hygroscopic moisture is comparably low ( $W_{hav} = 2.3\%$ ), which is in correspondence with low content of palagonite in the rocks of this group and with the absence of clayey minerals. Hyaloclastites of the group under consideration are weakly cemented ( $R_c = 2-13 \text{ MPa}$ ).

In general, hyaloclastites of **Group II** are similar to those of Group I but differ by a greater extent of palagonitization. As the latter advances, the color of the

rocks changes from dark to yellow and ochre. Fragments of volcanic glass are covered by “skirts” of palagonite, on the average 10  $\mu\text{m}$  or, less frequently, 20  $\mu\text{m}$  thick, forming a film-type cement (Fig. 4). It should be noted that micro cracks are formed transversely to the glass–palagonite interface. Palagonite also forms on the inner surface of some gas pores on the volcanic glass matrix and in feeder micro cracks. Closed gas cavities not connected by micro cracks to the interclastic space remain empty (Fig. 4). In thin sections, palagonite “skirts” are optically isotropic, although in some cases their outer layers manifest some signs of optical anisotropy indicating the onset of crystalline matter formation. No secondary minerals are observed in the interclastic space. Of all the rocks under consideration hyaloclastites of group II have the highest porosity ( $n = 45-57\%$ ) and permeability ( $K = (1.7-6.4) \times 10^3 \text{ mD}$ ) and the lowest density (Table 2). Compared to group I, rocks from group II have a slightly reduced density and solid phase density and an increased permeability. This tendency is in favor of volcanic glass substitution by palagonite in equal vol-

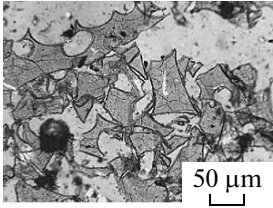
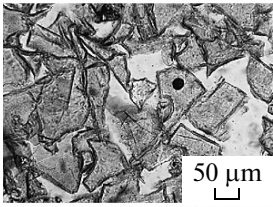
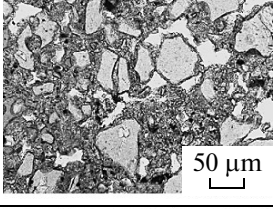
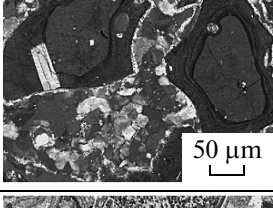
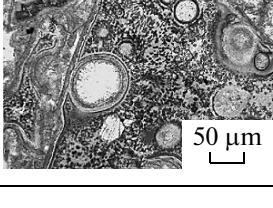
Group	Thin Section	Cement type	Secondary minerals
I		Contact	Optically isotropic gel-palagonite
II		Film	Optically isotropic palagonite Anisotropic stratified palagonite
III		Film-porous	Palagonite-smectite
IV		Porous	Palagonite Smectite olites
V		Porous-basal	Corrensite (chlorite) Calcite Prenite Clinzoisite

Fig. 4. Stages of hyaloclastite transformation with the growth of the level of conversion.

umes (with the same boundaries) rather than palagonite deposition on the glass matrix. According to Hay and Iijima [1968], the density of palagonite is 1.93–2.14 g/cm<sup>3</sup>, whereas the density of basalt glass is 2.75–2.85 g/cm<sup>3</sup>. Therefore, the substitution of dense glass for more porous palagonite leads to reduced rock density and increased porosity at this stage of transformation.

Effective air-filled and general porosities are similar, i.e., practically all pores are interconnected ( $n_{\text{air}}/n = 0.8–0.96$ ). The effective water-filled porosity is on the average 30% lower than the air-filled porosity. The hygroscopic moisture of hyaloclastites at this stage is notably increased ( $W_{\text{hav}} = 6.5\%$ ) due to an increase in palagonite content. Hyaloclastites remain weakly cemented as indicated by low values of elastic-

ity-strength characteristics ( $R_c = 2–10$  MPa;  $V_p = 0.9–1.55$  km/s).

Most hyaloclastites of **Group III** were generated during the most recent glaciation and underwent no burial, however some samples allocated to this group by cluster analysis belong to a thickness dated 2 million years ago, which was buried at a depth of 700–1000 m. Hyaloclastites are mainly ochre–yellow. The surfaces of glass fragments and vesicle walls are covered with “skirts” of palagonite, while the inner parts adjoining the glass are composed of optically isotropic gel-palagonite and the outer layers of optically anisotropic fibropalagonite (the progenitor of smectite). Small vesicles  $\leq 0.05$  mm in diameter are filled with palagonite, large pores ( $\geq 0.1$  mm in diameter) are partially filled, and the central parts are empty. The interclastic space is filled with palagonite or smectite forming a porous-type cement (Fig. 4).

Filling of interclastic space and formation of porous-type cement result in rock consolidation ( $\rho = 1.53–1.85$  g/cm<sup>3</sup>) and strengthening ( $R_c = 8–37$  MPa, on the average 19 MPa), an increase of  $V_p$  to 1.3–2.7 km/s and a respective decrease of porosity ( $n = 31–45\%$ , on the average 37%) and permeability ( $K = (0.4–9.5) \times 10^2$  mD, on the average  $6.1 \times 10^2$  mD) (Table 2). The general porosity and effective air-filled and water-filled porosities differ significantly. The effective air-filled porosity is approximately 20% lower than the general porosity and 20% higher than the effective water-filled porosity, indicating a decrease in the volume of open pores at this stage of transformations. The hygroscopic moisture increases to as high as 10.6% ( $W_{\text{hav}} = 5.6\%$ ) due to the substantial contents of palagonite and smectite in the rocks. Solid phase density decreases ( $\rho_s = 2.49–2.8$  g/cm<sup>3</sup>, on the average 2.66 g/cm<sup>3</sup>).

**Group 4** is heterogeneous in terms of geology, including hyaloclastites of different ages (from the most recent glaciation back to 1.7–2.0 Ma ago) and burial depth (from 0 to 700 m). Hyaloclastites from this group can be distinguished by the presence of several generations of palagonite and secondary authigenic minerals in the pores, such as zeolites, calcite, and smectite (Figs. 4, 5). Palagonite is represented by both isotropic and anisotropic types, i.e., it is partly recrystallized into smectite, as detected by X-ray analysis. A detailed examination of the clayey component showed that it is either trioctahedral smectite (saponite) or a mixed-layered formation of smectite–chlorite composition, with the prevalence of smectite component. Zeolites are represented by two basic generations, viz., rhombic crystals of shabazite forming in the interclastic space and radial aggregates of phillipsite growing on the glass fragments) (Fig. 4). In some samples analcite occurs, whose grains form chains along the surface of glass fragments (Fig. 5). The interclastic space is filled practically in full with secondary minerals (zeolites and smectite). Glass fragments remain

partly unaltered, whereas vesicles are completely filled with zeolites and clayey minerals. In this case, micro cracks cleaving through the glass fragments are likely to serve as pathways to the pores for fluids.

Hyaloclastites of group IV are significantly denser ( $\rho = 1.85\text{--}2.34\text{ g/cm}^3$ , on the average  $2.03\text{ g/cm}^3$ ) and more resistant ( $R_c = 40\text{--}111\text{ MPa}$ ) as compared to the previous groups (Table 2). Intense generation of authigenic minerals in the interclastic space and vesicles leads to a substantial decrease in porosity ( $n = 14\text{--}27\%$ , on the average  $21\%$ ) and permeability ( $K = 0.23\text{--}203\text{ mD}$ , on the average  $55\text{ mD}$ ). Effective air-filled porosity is considerably lower than general porosity: only 60% pores are permeable for air.

Of interest is the fact that this stage of transformation is characterized by an unusual  $n_{\text{air}}$  to  $n_{\text{water}}$  ratio: effective air-filled porosity is equal or even lower than effective water-filled porosity. Such an unusual ratio is likely to be due to high content of smectite, a clayey mineral with a specific microstructure capable of absorbing plenty of water and swelling. Thus, on the one hand,  $n_{\text{water}}$  increases due to high water absorption, and, on the other hand,  $n_{\text{air}}$  decreases because smectite does not let air pass.

High smectite content corresponds to high  $W_h = 3.3\text{--}10.4\%$  (on the average  $5.8\%$ ). The solid phase density is low ( $\rho_s = 2.45\text{--}2.75\text{ g/cm}^3$ , on the average  $2.57\text{ g/cm}^3$ ), due to basalt glass transformation and formation of zeolites having low densities ( $\rho = 2.1\text{--}2.2\text{ g/cm}^3$ ). The values  $V_p = 1.3\text{--}2.95\text{ km/s}$  are not much higher than for previous groups, despite their comparatively low porosity and higher density. Low  $V_p$  values are obviously due to high rates of zeolitization. In earlier studies intense zeolitization of tuffs was shown to result in a notable decrease of  $V_p$  [Lagygin et al., 2000].

Allocation of hyaloclastites of different ages and burial depths to the same group IV is obviously conditioned by the following. As is known, zeolitization can occur in different geological conditions: in subsurface conditions as a result of diluvial hydrothermal activity or under burial of volcanogenic thickness of zeolite metamorphic facies, which are abundant in Iceland. In both cases the composition of hyaloclastites undergoes similar transformations, which explains the homogeneity by properties.

**Group 5** includes hyaloclastites of the Pliocene thickness (2–2.5 million years) buried to a depth of 1000 m. Spatially the Pliocene thickness is the most distant from the neovolcanic zone. Light-gray rocks of this type are strongly transformed and closely cemented. The interclastic space, cracks, and vesicles are filled with authigenic minerals (Fig. 4). Unlike the previous groups, the fragments of volcanic glass are substantially altered. The secondary minerals are mainly chlorite or corrensite, calcite, clinozoisite, prenite, quartz.

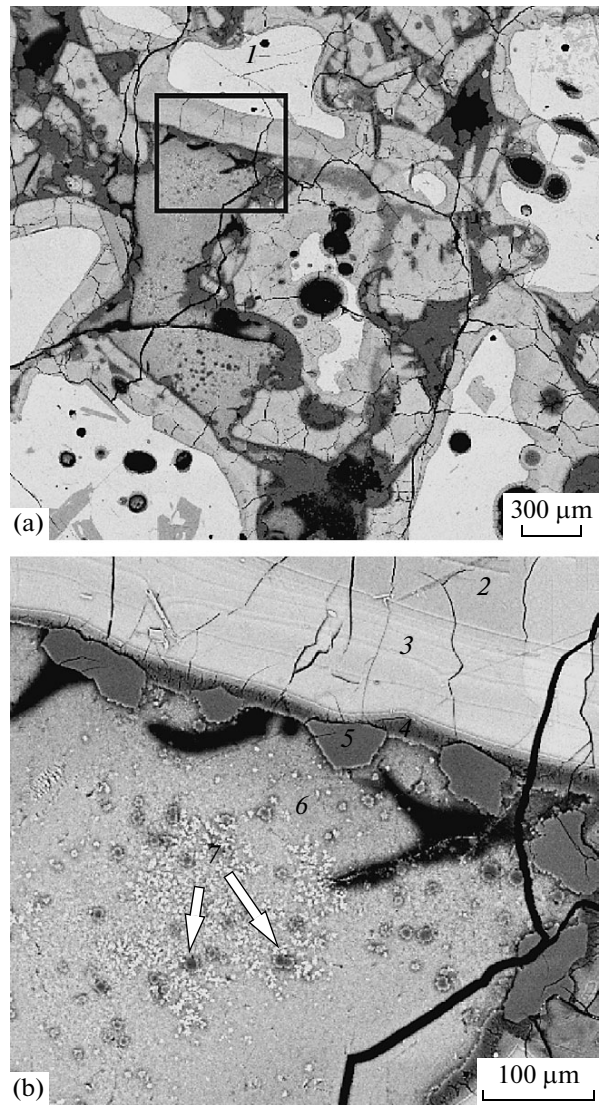


**Fig. 5.** Secondary hyaloclastite transformations (electron microscopy): 1, unaltered glass; 2, X-ray amorphous palagonite; 3, layered palagonite; 4, saponite; 5, analcite; 6, chabazite; 7, saponite.

As a result of a greater degree of conversion, hyaloclastites from this group are characterized by the highest structural density ( $\rho_{\text{av}} = 2.13\text{ g/cm}^3$ ) and high strength ( $R_p = 48\text{--}100\text{ MPa}$ , on the average  $70\text{ MPa}$ ) despite a slight increase in porosity as compared with the preceding stage ( $n = 25\text{--}43\%$ , on the average  $33\%$ ). A possible explanation is found in the secondary porosity formed as a result of recrystallization of volcanic glass and its replacement with corrensite. However, pores are ultra small and do not allow fluids to pass, which explains the low permeability of these rocks ( $K = 10^{-3}\text{--}6.1 \times 10^{-2}\text{ mD}$ ). The  $n_{\text{air}}/n$  ratio indicates that, similarly to the preceding group, about 60% of all pores are interconnected. The unusual  $n_{\text{air}}/n_{\text{water}}$  ratio  $\leq 1$  characteristic for the preceding group also

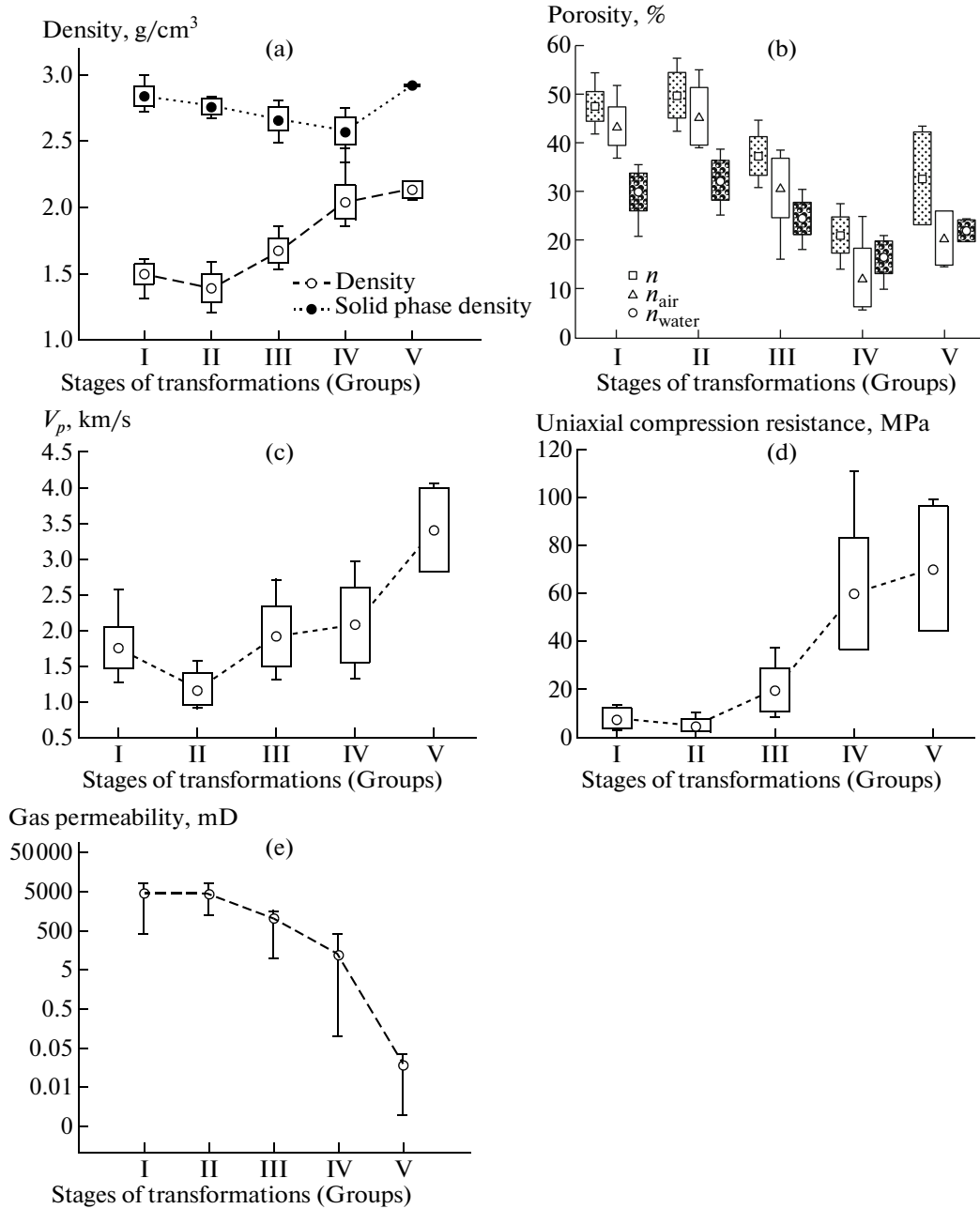


**Fig. 6.** Hyaloclastite properties vs. stages of transformation: (a) density and solid phase density; (b) porosity; (c) velocity of longitudinal waves propagation; (d) uniaxial compression resistance; (e) gas permeability. These stages (I–V) are described in the text. On the curves: average values for indicators are plotted as dots, standard deviations, as boxes, and minimal and maximum values, as “whiskers.”

holds for the rocks of Group 5. Gradual conversion of smectite into chlorite is accompanied by a decrease of  $W_h$  to 2.3%. Solid phase density increases notably, to  $2.92 \text{ g/cm}^3$ , as a result of generation of the minerals such as chlorite and clinozoisite.

**Features of hyaloclastite lithification.** Analysis of the collection of samples as a whole and each group separately indicates that the hyaloclastites under investigation during lithogenesis undergo a sequence

of mineral transformations: gel-palagonite → stratified palagonite → smectite and zeolites → corrensite/chlorite, calcite, prenite, and clinozoisite. The aforementioned transformations are accompanied by a successive shift in the type of cement: contact → film → porous → secondary porous-basal with rapid recrystallization of primary material (Fig. 4). The structure of the pore space also changes: interclastic pores and gas cavities are gradually filled with second-

ary minerals, the portion of connecting pores decreases and so does permeability. However, at this stage of investigation it is not possible to analyze and estimate the contribution of particular factors and conditions of hyaloclastite generation and transformation (weathering, groundwater, temperature, glacial conditions, etc.).

In general, a natural increase in elasticity–density and strength characteristics and a decrease in porosity and permeability can be observed in hyaloclastites in the course of postgenetic transformations with an increase in burial depth (from 0 to 1000 m) and age (from the most recent glaciation <300 years ago to 2–2.5 million years ago). Hyaloclastites become much more consolidated, viz., their density increases from 1.3–1.5 to 2.2–2.3 g/cm<sup>3</sup>, whereas the porosity decreases from 50–55 to 20–30% (Figs. 6a, 6b).

Figure 6 illustrates the general tendency in porosity changes in the course of postgenetic alterations of hyaloclastite. The porosity and permeability of hyaloclastites generally decrease during their lithification from practically unaltered weakly palagonitized varieties with loose contact-film cement ( $n = 45–50\%$ ,  $K \sim 10^3$  mD) to rapidly altered rocks with authigenic minerals (zeolites, calcite, and clays) filling the interclastic space and substituting a larger part of primary volcanic glass ( $n = 20–30\%$ ,  $K \sim 10^{-3}$  mD)

However, the noted tendency was found to have some deviations. In particular, palagonite ensures initial cementation of unbounded glass fragments and their transformation into consolidated rock characterized by high porosity and permeability. Further formation of porous palagonite replacing dense volcanic glass on the rims (without changing the volume) leads to a slight increase of porosity and permeability, which is not in line with the noted postgenetic dynamics of these parameters. The increase in permeability is likely to be associated with the appearance of micro cracks during palagonite generation. At the subsequent stages of rock transformation a natural reduction of permeability to  $\sim 10^{-3}$  mD is observed in the most converted ancient varieties. During progressive palagonitization and subsequent smectitization and zeolitization, the porosity also decreases. At the last stage, the general porosity increases due to the formation of secondary pores during substitution of dense volcanic glass for porous corrensite. However, small new pores typical for corrensite are impermeable to fluids and do not enhance rock permeability.

In the process of lithogenesis the structure of pore space changes, as can be indirectly judged from the  $n$ ,  $n_{\text{air}}$  and  $n_{\text{water}}$  proportions. As noted, intensely converted hyaloclastites are characterized by the unusual relation  $n_{\text{air}} \leq n_{\text{water}}$ , which results from extensive generation of clayey minerals (smectite, corrensite) which are impermeable for air but have high absorptive capacity for water (Fig. 6b).

As a result of hyaloclastite cementation, enhancement of binding between fragments and filling of pore

space with secondary minerals, the strength of hyaloclastites increases by two orders, from a few MPa to 100 MPa (Fig. 6d); values  $V_p$  rise to 3.5–4 from 1.5–2 km/s (Fig. 6c). During lithification with a decrease of rock porosity, heat conductivity increases from extremely low values of 0.3–0.4 W/m K for weakly cemented Upper Pleistocene hyaloclastites to 0.9–1.3 W/m K for the Pliocene lithified rocks.

## CONCLUSIONS

1. Hyaloclastites are generally highly porous, permeable, low-strength, hygroscopic grounds. Depending on the extent of lithification, they can be classified with both rock and semirock groups.

2. Palagonitization is a major contributor to the transformation of loose hyaloclastite deposits into rock grounds.

3. Mineral transformation of hyaloclastites during lithogenesis was shown to proceed in the following order: X-ray amorphous -palagonite → stratified palagonite → smectite and zeolites → corrensite/chlorite, calcite, prenite, and clinzoisite.

4. During lithogenesis, the structure of hyaloclastites undergoes changes accompanied by a successive switch of the cement type: contact → film → porous → secondary porous-basal with rapid recrystallization of primary materials. The structure of the pore space also changes: interclastic pores and gas cavities eventually become filled with secondary minerals; the portion of interconnected pores decreases and so does permeability. Under intense transformation of volcanic glass secondary porosity occurs, which, however, does not enhance permeability.

5. In the general case, the elasticity–density and strength characteristics of hyaloclastites increase in a predictable manner, whereas porosity and permeability decrease during postgenetic transformations with the aging of hyaloclastite thickness and an increase in the depth of its burial.

6. Hyaloclastites are characterized by abnormally low heat conductivity due to their high porosity and clastic structure, with the most fragment being weakly cemented.

7. Intensely altered hyaloclastites are characterized by an unusual relationship  $n_{\text{air}} \leq n_{\text{water}}$  due to extensive generation of clayey minerals (smectite and corrensite) that are impermeable to air but highly absorptive to water.

## ACKNOWLEDGMENTS

This work was supported by RFFI grant no. 07-05-00118-a.

## REFERENCES

1. Crovisier, J.-L., Honnorez, J., Fritz, B., and Petit, J.-C., Dissolution of Subglacial Volcanic Glasses from Ice-

- land: Laboratory Study and Modeling, *Appl. Geochem.*, 1992, Suppl. issue 1, pp. 55–81.
2. Dortman, N.B., *Fizicheskie svoistva gornykh porod i noleznykh iskopaemykh (petrofizika): Spravochnik geofizika* (Physical Properties of Mounting Rocks and Minerals (Petrophysics): Handbook for Geophysicist), Moscow: Nedra, 1984.
  3. Genshaft, Yu.S. and Saltykovskii, A.Ya., *Islandiya: glubinnoe stroenie, evolyutsiya i intruzivnyi magmatizm* (Iceland: Subsurface Structure, Evolution and Intrusive Magmatism), Moscow: GEOS, 1999.
  4. Geptner, A.R., Palagonite and the Process of Palagonite Formation, *Litol. Miner. Res.*, 1977, no. 5, pp. 113–129.
  5. Geptner, A.R., Selezneva, M.A., Smelov, S.B., and Liskun, I.G., Formation Condition and Initial Stages of Variation for Basalt Glass, *Litol. Polezn. Iskop.*, 1984, no. 4, pp. 44–61.
  6. GOST (State Standard) no. 26450.2–85: *Rocks. The Ways to Determine the Coefficient of Absolute Gas Permeability under Stationary and Nonstationary Filtration*, Moscow: Gosudarstvennyi komitet USSR po standartam, 1985.
  7. *Gruntovedenie* (Soil Science), Trofimov, V.T., Ed., Moscow: MGU, 2005.
  8. Hay, R.L. and Iijima, A., Nature and Origin of Palagonite Tuffs of the Honolulu Group on Oahy, Hawaii, *Geol. Soc. Amer. Met.*, 1968, vol. 116, pp. 338–376.
  9. Jakobsson, S. and Moore, J., Hydrothermal Minerals and Alterations Rates at Surtsey Volcano, Iceland, *Geol. Soc. Amer. Bull.*, 1986, vol. 116, pp. 338–376.
  10. Jones, J.C., Intraglacial Volcanoes of the Laugarvatn Region, Southwest Iceland, *J. Geol.*, 1970, vol. 78, no. 2, pp. 127–139.
  11. Frolova, J., Ladygin, V., Franzson, H., Sigurdsson, O., et al., Petrophysical Properties of Fresh to Mildly Altered Hyaloclastite Tuffs, *Proc. World Geothermal Congr.*, Antalya, Apr. 24–29, 2005.
  12. Ladygin, V., Frolova, J., and Rychagov, S., Formation of Composition and Petrophysical Properties of Hydrothermally Altered Rocks in Geothermal Reservoir, *Proc. of the World Geothermal Congr.*, Kyushu–Tohoku, 2000, pp. 2695–2699.
  13. Popov, V.G., Petrunin, G.I., Pugina, L.M., et al., Consolidation Degree (Lithification) Effect onto Heat Transfer Parameters for Tuffs (by Example of Iceland Tuffs), *Tez. dokl. 8–e geofizicheskie chteniya im. V.V. Fedynskogo 2–4 marta 2006 g.* (Proc. 8th V. V. Fedynskii Geophysical Meetings Mar. 2–4, 2006), Moscow, 2006, pp. 88–89.
  14. Saemundsson, K., Outline of the Geology of Iceland, *Jokull*, 1979, no. 29, pp. 7–28.
  15. Schiffman, P., Spero, H.J., Southard, R.J., and Swanson, D.A., Control on Palagonitization Versus Petrogenic Weathering of Basaltic Tephra: Evidence from the Consolidation and Geochemistry of the Keanakako'i Ash Member, Kilauea Volcano. Geochemistry, Geophysics, Geosystems, *Electron. J. Earth Sci.*, 2000, vol. 1.
  16. Stroncik, N.A. and Shmincke, H.-U., Evolution of Palagonite: Crystallization, Chemical Changes, and Element Budget. Geochemistry, Geophysics, Geosystems, *Electron. J. Earth Sci.*, 2001, vol. 2.
  17. Thorseth, I.H., Furnes, H., Tumyr, O., A Textural and Chemical Study of Iceland Palagonite of Varied Composition and Its Bearing on the Mechanism of the Glass–Palagonite Transformation, *Cheochim. et Cosmochim. Acta*, 1992, vol. 56, no. 2, pp. 845–850.
  18. Trofimov, V.T. and Korolev, V.A., Ways to Study Soils' Physical Properties, in *Praktikum po gruntovedeniyu* (Case–Study on Soil Science), Moscow, 1993, pp. 168–214.
  19. Zhou, Z. and Fyfe, W.S., Palagonitization of Basaltic Glass from DSDP Site 335, Leg 37: Textures, Chemical Composition, and Mechanism of Formation, *Amer. Mineral.*, 1989, vol. 74, pp. 1045–1053.